Pillar[5]arene-based amphiphilic supramolecular brush copolymer: fabrication, controllable self-assembly and application in self-imaging targeted drug delivery

Guocan Yu,[a,c,‖] Run Zhao,[a,‖] Dan Wu,[b,‖] Fuwu Zhang,[c] Li Shao,[a] Jiong Zhou,[a] Jie Yang,[a] Guping Tang,[b] Xiaoyuan Chen,[c,*] and Feihe Huang[a,*]

[a] *State Key Laboratory of Chemical Engineering, Center for Chemistry of High-Performance & Novel Materials, Department of Chemistry, Zhejiang University, Hangzhou 310027, P. R. China. Email: fhuang@zju.edu.cn*

[b] *Department of Chemistry, Institute of Chemical Biology and Pharmaceutical Chemistry, Zhejiang University, Hangzhou 310027, P. R. China*

[c] *Laboratory of Molecular Imaging and Nanomedicine, National Institute of Biomedical Imaging and Bioengineering, National Institutes of Health, Bethesda, Maryland 20892, United States. Email: chenx5@mail.nih.gov*

‖ These authors contributed equally to this work.

Electronic Supplementary Information (17 pages)

1. Materials and methods

All reagents were commercially available and used as supplied without further purification. Solvents were either employed as purchased or dried according to procedures described in the literature. **M**,[S1] **PTPE**,[S2] **P5**,[S3] and **P5-PEG-Biotin**[S3] were prepared according to literature procedures. ^{1}H NMR and ^{13}C NMR spectra were recorded on a Bruker Avance-400 spectrometry. The 2D NOESY NMR spectrum was collected on a Bruker Avance DMX-500 spectrometer with internal standard TMS. Low-resolution electrospray ionization (LRESI) mass spectra were obtained on a Bruker Esquire 3000 plus mass spectrometer (Bruker-Franzen Analytik GmbH Bremen, Germany) equipped with an ESI interface and an ion trap analyzer. HRMS were obtained on a WATERS GCT Premier mass spectrometer. The melting points were collected on a SHPSIC WRS-2 automatic melting point apparatus. The fluorescence experiments were conducted on a RF-5301 spectrofluorophotometer (Shimadzu Corporation, Japan). Transmission electron microscopy (TEM) investigations were carried out on a HT-7700 instrument. Scanning electron microscopy (SEM) investigations were carried out on a Multimode 8 instrument. Molecular weights and distributions were determined by gel permeation chromatography (GPC) with a Waters 1515 pump and Waters 1515 differential refractive index detector (set at 30 °C).

TEM and DLS Studies. The nanostructures of the nanoparticles were revealed using TEM. TEM samples were prepared by drop-coating a solution onto a carbon-coated copper grid. TEM experiments were performed on a HT-7700 instrument. The corresponding solution was left to stand overnight and the insoluble precipitate was eliminated by using a microporous membrane before DLS tests. Dynamic light scattering (DLS) measurements were carried out using a 200 mW polarized laser source Nd:YAG (λ = 532 nm). The polarized scattered light was collected at 90° in a self-beating mode with a Hamamatsu R942/02 photomultiplier. The signals were sent to a Malvern 4700 submicrometer particle analyzer system.

DOX Loading and Release. PTPE (16.0 mg), **P5-PEG-Biotin** (71.7 mg), and DOX·HCl (50 mg) were dissolved in the mixture of water (10 mL) and THF (10 mL) in the presence of triethylamine (TEA). After stirring in the dark for 24 h, THF was evaporated by N_2 flow. The DOX-loaded **SNPs** were purified by dialysis (molecular weight cut-off 3000) in distilled water until the water outside the dialysis bag exhibited negligible DOX fluorescence. The amount of unloaded DOX in the dialysate was quantitatively measured by UV-Vis spectrophotometry at 480 nm. The DOX encapsulation was calculated by the following equations:

$$\text{Encapsulation Efficiency (\%)} = (m_{\text{DOX-loaded}}/m_{\text{DOX}})*100$$

$m_{\text{DOX-loaded}}$ and m_{DOX} are masses of DOX encapsulated in the DOX-loaded **SNPs** and DOX added,

respectively.

The DOX release from the DOX-loaded **SNPs** was studied in different pH buffer solutions. A dialysis bag with 2 mL of the DOX-loaded **SNPs** solution was added into the corresponding release medium (18 mL) at 37 °C. At specified time intervals, the concentration of DOX was determined by UV-Vis spectrophotometry.

For reduction-triggered release studies, the DOX-loaded **SNPs** were dissolved in 2 mL of a phosphate buffer solution in the absence or presence of $Na_2S_2O_4$ sealed in a dialysis bag with a molecular weight cut-off of 3 kDa. The dialysis apparatus was agitated on an orbital shaker at 100 rpm at 37 °C. At designated time intervals, 1 mL of medium was taken out from the 25 mL solution out of the dialysis bag for UV detection and was then put back to the original system. The DOX concentration in the solution was calculated based on the standard curve calibrated with a DOX solution with a known concentration.

Cell Cultures. HeLa and HEK293 cells were purchased from the American Type Culture Collection (ATCC, Rockville MD) and cultured in Dulbecco's modified Eagle's medium (DMEM) containing 10% fetal bovine serum (FBS, MesGen, Shanghai, China) and 1% penicillin/streptomycin. Cells grew as a monolayer and were detached upon confluence using trypsin (0.5% *w*/*v* in PBS). The cells were harvested from the cell culture medium by incubating in a trypsin solution for 5 min. The cells were centrifuged, and the supernatant was discarded. A 3 mL portion of serum-supplemented DMEM was added to neutralize any residual trypsin. The cells were resuspended in serum-supplemented DMEM at a concentration of 1×10^4 cells/mL. Cells were cultured at 37 °C and 5% CO_2.

Evaluation of Cytotoxicity. The cytotoxicities of free NPs, DOX·HCl, and the DOX-loaded **SNPs** against HeLa and HEK293 cells with or without the pretreatment of biotin were determined by 3-(4′,5′-dimethylthiazol-2′-yl)-2,5-diphenyl tetrazolium bromide (MTT) assays in a 96-well cell culture plate. All solutions were sterilized by filtration with a 0.22 μm filter before tests. HeLa and HEK293 cells were seeded at a density of 1×10^4 cells/well in a 96-well plate, and incubated for 24 h for attachment. Cells were then incubated with free NPs, DOX·HCl, or the DOX-loaded **SNPs** at various concentrations for 24 h. After washing the cells with PBS buffer, 20 μL of a MTT solution (5 mg/mL) were added to each well. After 4 h of incubation at 37 °C, the MTT solution was removed, and the insoluble formazan crystals that formed were dissolved in 100 μL of dimethylsulfoxide (DMSO). The absorbance of the formazan product was measured at 570 nm using a spectrophotometer (Bio-Rad Model 680). Untreated cells in media were used as a control. All experiments were carried out with five replicates.

***In Vitro* Cell Accumulation of DOX Determined by Flow Cytometry.** Cellular uptake of the DOX-loaded **SNPs** was measured by flow cytometry. HeLa and HEK293 cells were seeded at a density of 3.00

$\times 10^5$ cells/well in 12-well cell culture plates. The cells were left to grow for 24 h in DMEM media containing 10% FBS at 37 °C in 5% CO_2 atmosphere. After 24 h, the DOX-loaded **SNPs** (the concentration of DOX was 5.00 μM) were added to the wells and the cells were incubated for 30 min, 1 h, 2 h, and 4 h, respectively. Following incubation, cells were rinsed twice with PBS to remove residual DOX-loaded **SNPs**. Cells were harvested by trypsinization and resuspended in 500 μL of PBS for flow cytometry analysis using the FACS Calibur flow cytometer (BD Facsealibur). Data shown in this paper are the mean fluorescent signal for 1.00×10^4 cells. Cells without any treatment were used as a control. Data was analyzed using the FlowJo software.

***In Vitro* Cell Accumulation Determined by Confocal Laser Scanning Microscopy.** HeLa and HEK293 cells were treated with DOX-loaded **SNPs** (the concentration of DOX was 5.00 μM) in the culture medium at 37 °C for 0.5 h, 2 h, and 4 h, respectively. The cells were washed three times with PBS, fixed with fresh 4.0% formaldehyde at room temperature for 15 min, and washed with PBS for two times. The images were taken using a LSM-510 confocal laser scanning microscope (Zeiss, Germany) (100 × oil objective, 405/488 nm excitation).

Animals and Tumor Models. Female BALB/c nude mice (4 weeks old, ~20 g body weight) were purchased from Zhejiang Academy of Medical Sciences and maintained in a pathogen-free environment under controlled temperature (24 °C). Animal care and handling procedures were in agreement with the guidelines evaluated and approved by the ethics committee of Zhejiang University. Study protocols involving animals were approved by the Zhejiang University Animal Care and Use Committee. The female nude mice were injected subcutaneously in the right flank region with 200 μL of cell suspension containing 5×10^6 HeLa cells. The tumors were allowed to grow to ~100 mm^3 before experimentation. The tumor volume was calculated as (tumor length) × (tumor width)^2/2. Relative tumor volumes were calculated as V/V_0 (V_0 was the tumor volume when the treatment was initiated).

Pharmacokinetics and Biodistribution. For pharmacokinetic studies, the mice were randomly divided into two groups (n = 3). The aqueous solutions of free DOX·HCl and the DOX-loaded **SNPs** were *i.v.* injected at a dose of 5 mg/kg. The blood samples (0.2 mL) were taken from retro-orbital sinus at desired time after injection. The plasma was obtained by centrifugation at 10000 rpm for 15 min to isolate the plasma, and the amount of DOX in the plasma was assayed by HPLC.

The DOX concentrations in the tumor tissues and organs were analyzed by HPLC. 200 μL of 10% (*w*/*v*) tissue homogenate were added with 20 μL of daunorubicin (20 μg/mL) and 100 μL of 0.2 M PBS (pH 7.8). The above mixture was subsequently extracted with chloroform/isopropanol (4:1, *v*/*v*) by vortex mixing for 3 minute. After centrifugation (10000 rpm, 5 min), the organic phase was separated and

evaporated to dryness under a stream of nitrogen. The residue was dissolved in 200 μL of the mobile phase (methanol/water/acetic acid = 65:35:2, *v*/*v*/*v*). After centrifugation (10000 rpm, 5 min), the supernatant was collected for HPLC analysis.

***In Vivo* Antitumor Efficacy Evaluation.** The nude mice were divided into three treatment groups randomly (n = 7), when the mean tumor volume reached about 100 mm^3 and this day was set as day 0. Mice were administered intravenously with PBS, free DOX, and the DOX-loaded **SNPs** at dose of 5 mg DOX/kg body weight every 3 days for four times. Tumor volume and body weight were measured every 3 days. The tumor inhibition study was stopped on the 21^{st} day and the survival rate study was stopped on the 30^{th} day.

Tissue Immunohistological Evaluation. In the histological assay, the heart, liver, spleen, lung, kidney and tumor tissues were fixed in 4% paraformaldehyde for 24 h. The specimens were dehydrated in graded ethanol, embedded in paraffin, and cut into 5 mm thick sections. The fixed sections were deparaffinized and hydrated according to a standard protocol and stained with hematoxylin and eosin (H&E) for microscopic observation. Apoptosis of the tumor cells in the mice after treatments was determined by the TUNEL method according to the manufacturer's instructions. The cell proliferations in tumor tissues were measured by anti-Ki67 monoclonal antibody according to the manufacturer's instructions.

Statistical analysis. Data are presented as the mean ± standard deviation (SD). Statistical analysis of data was performed with one-way analysis of variance (ANOVA). The level of significance was defined at $*p < 0.05$, $**p < 0.01$.

2. *Synthesis of **PTPE***

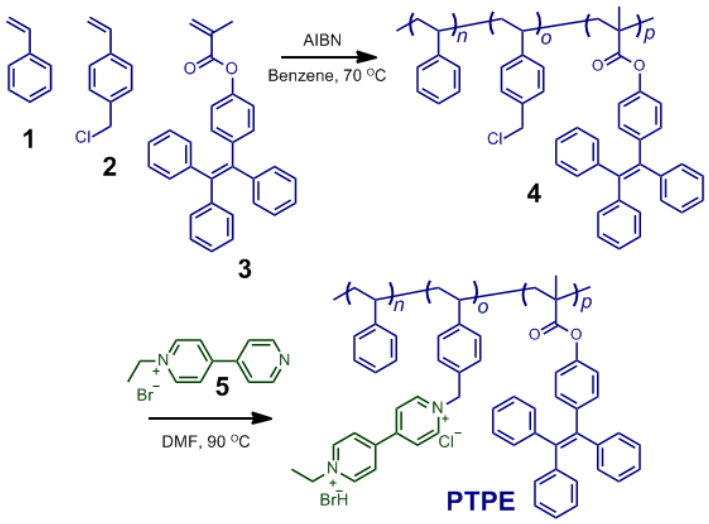

Scheme S1. Synthetic route to **PTPE**.

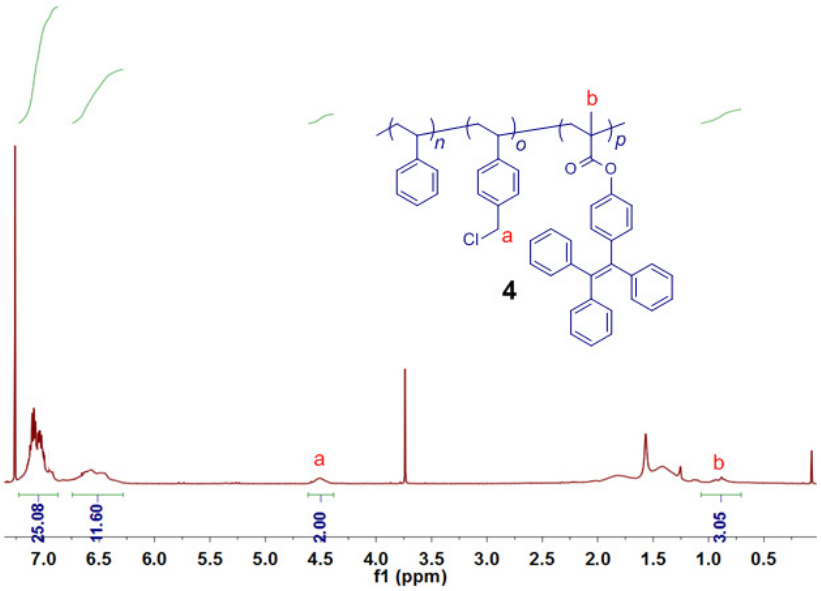

Fig. S1 ^{1}H NMR spectrum (400 MHz, chloroform-*d*, room temperature) of **4**.

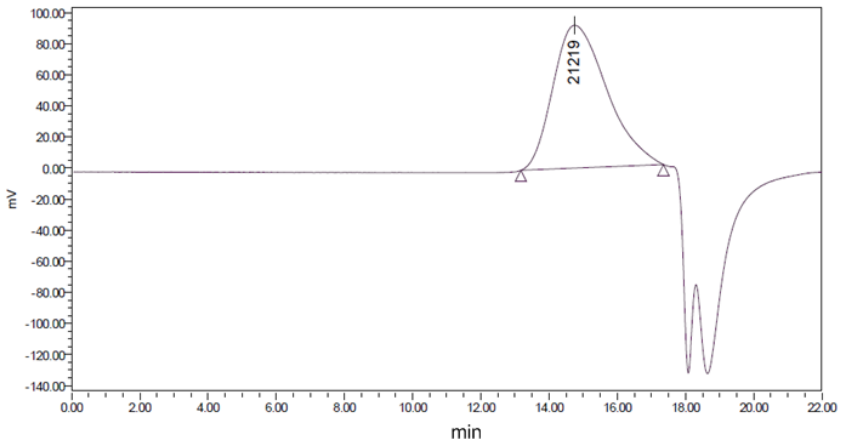

M_n	M_w	M_p	M_z	PDI
12288	21138	21219	31782	1.72

Fig. S2 GPC analysis of polymer **4** using conventional calculations, with polystyrene standards and DMF as the solvent.

The ratio of *p*/*o* was (3.05/3)/(2/2), namely 1.03/1, as calculated based on the integrations of the peaks of H_b and H_a, and *n*/*o* was 2.72/1 as calculated based on the integrations of peaks of aromatic protons. Therefore, the ratio of *n*/*o*/*p* was 2.72/1/1.03 for polymer **4**. According to M_n and the ratio of *n*/*o*/*p*, it can be calculated that the values of *n*, *o*, and *p* were 38, 14 and 14, respectively.

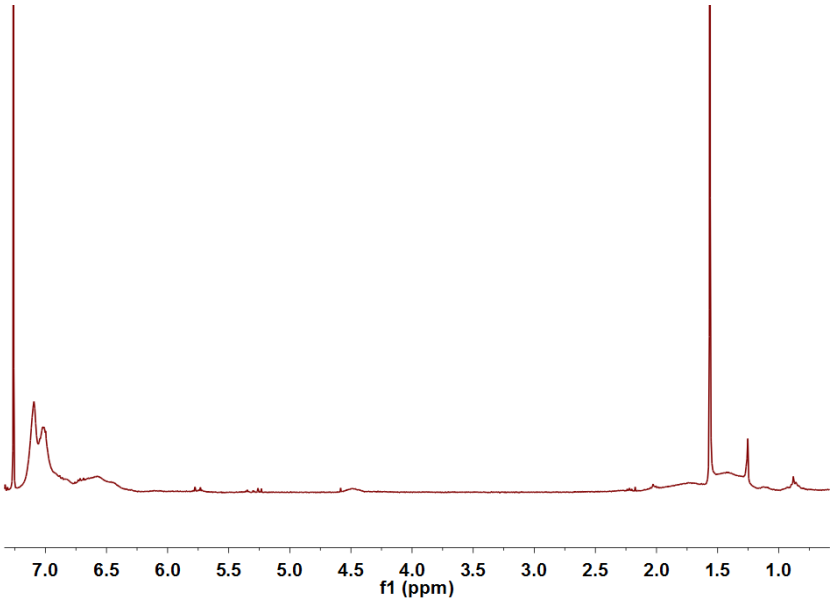

Fig. S3 ^{1}H NMR spectrum (400 MHz, chloroform-*d*, room temperature) of **PTPE**.

3. Investigations of the host–guest interactions

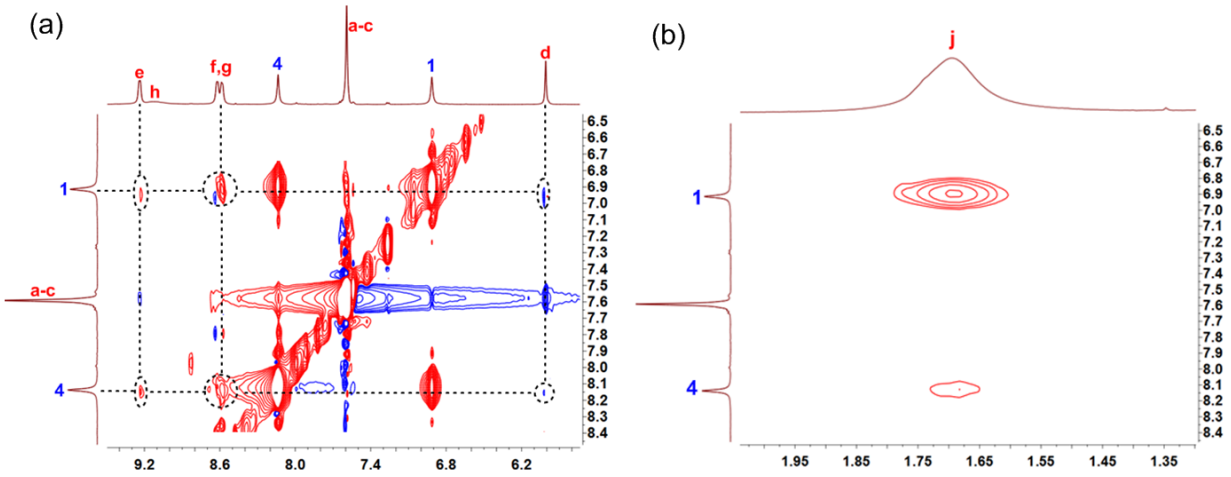

Fig. S4 2D NOESY NMR spectrum (500 MHz, D_2O, 295 K) of **P5** (10.0 mM) and **M** (30.0 mM).

To determine the stoichiometry and association constant for the complexation between **P5** and **M** (or $\mathbf{M}^{\cdot+}$), fluorescence titration experiments were done with solutions which had a constant concentration of **P5** (1.00×10^{-5} M) and varying concentrations of **M** (or $\mathbf{M}^{\cdot+}$). By a non-linear curve-fitting method, the association constant (K_a) of **P5**⊃**M** (or $\mathbf{M}^{\cdot+}$) was estimated. By a mole ratio plot, 1:1 stoichiometry was obtained for the complexation between **P5** and **M** (or $\mathbf{M}^{\cdot+}$).

The non-linear curve-fittings were based on the equation:

$$\Delta F = (\Delta F_\infty/[H]_0)\ (0.5[G]_0 + 0.5([H]_0+1/K_a) - (0.5\ ([G]_0^2 + (2[G]_0(1/K_a - [H]_0)) + (1/K_a + [H]_0)^2)^{0.5}))$$

where ΔF is the fluorescence intensity changes at 330 nm at $[H]_0$, ΔF_∞ is the fluorescence intensity changes at 326 nm when **P5** is completely complexed, $[G]_0$ is the initial concentration of **M** (or $\mathbf{M}^{\cdot+}$), and $[H]_0$ is the fixed initial concentration of **P5**.[S4]

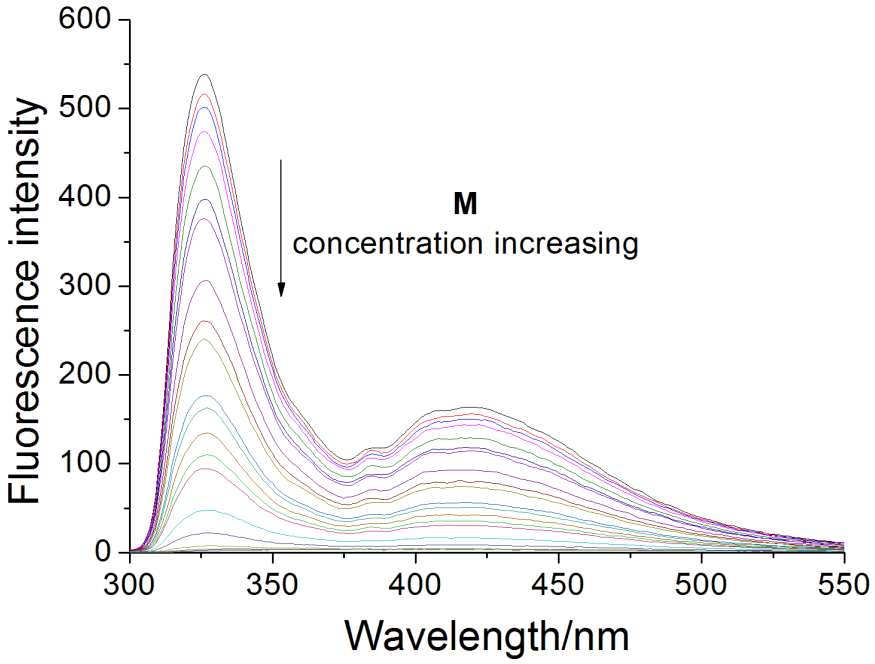

Fig. S5 Fluorescence spectra of **P5** (1.00×10^{-4} M) in water at room temperature with different concentrations of **M** at room temperature.

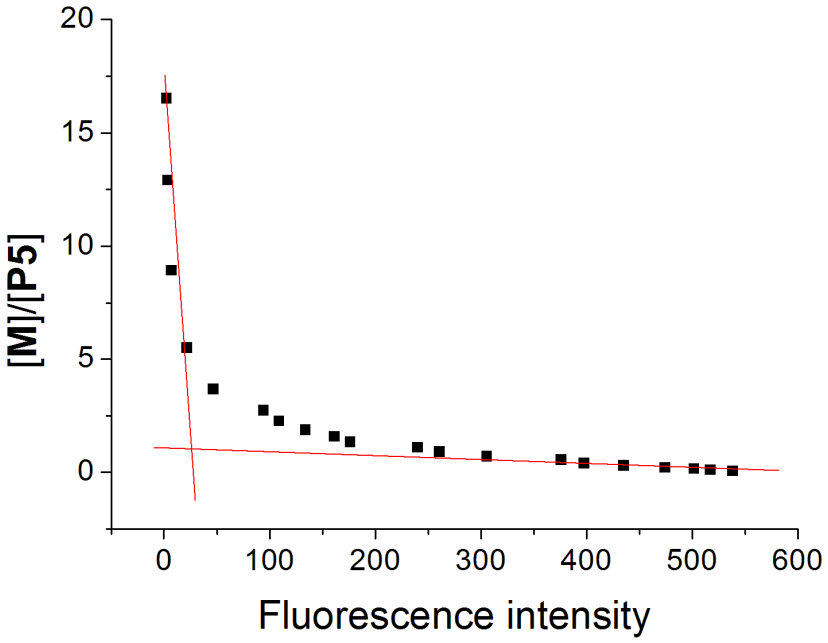

Fig. S6 Mole ratio plot for **P5** and **M** in water, indicating a 1:1 stoichiometry.

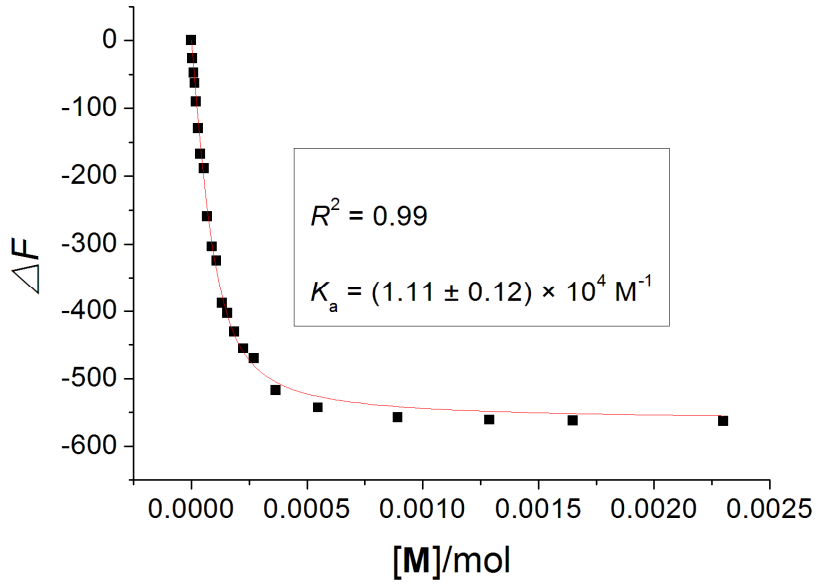

Fig. S7 Fluorescence intensity changes of **P5** in water upon addition of **M**. The red solid line was obtained from the non-linear curve-fitting using the above equation.

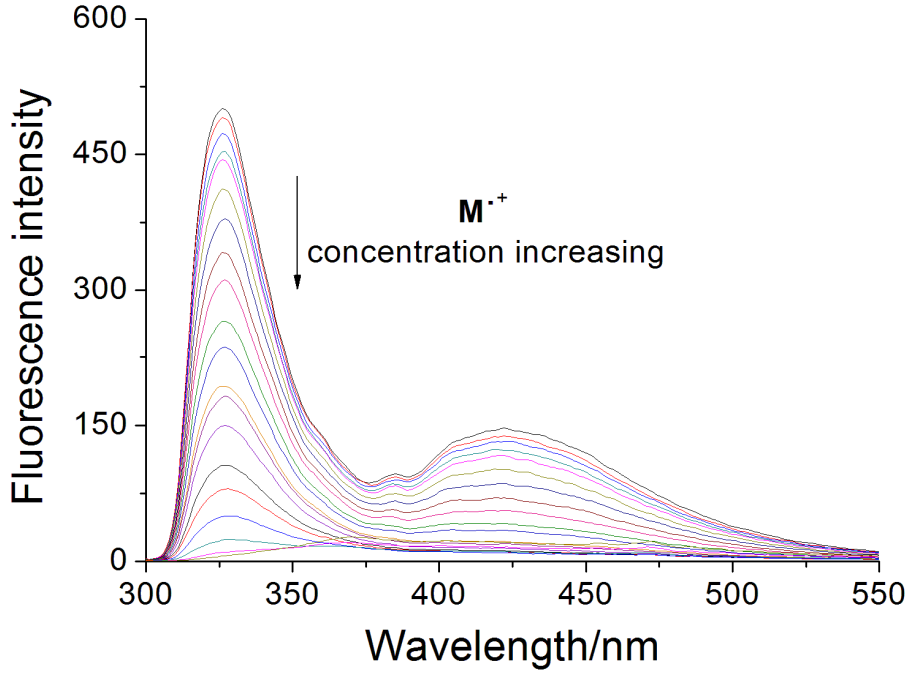

Fig. S8 Fluorescence spectra of **P5** (1.00×10^{-4} M) in water at room temperature with different concentrations of $\mathbf{M}^{\cdot+}$ at room temperature.

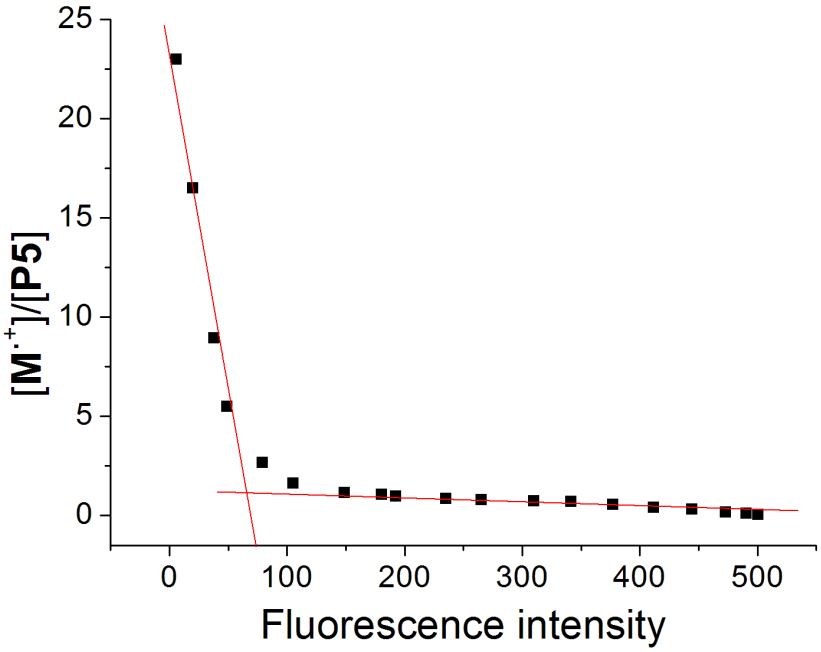

Fig. S9 Mole ratio plot for **P5** and $\mathbf{M}^{\cdot+}$ in water, indicating a 1:1 stoichiometry.

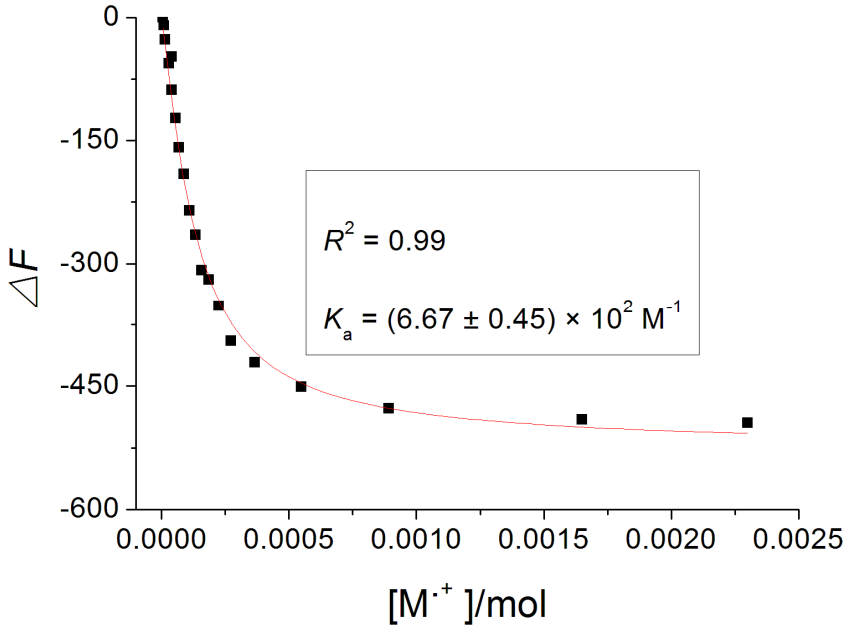

Fig. S10 Fluorescence intensity changes of **P5** in water upon addition of $\mathbf{M}^{\cdot+}$. The red solid line was obtained from the non-linear curve-fitting using the above equation.

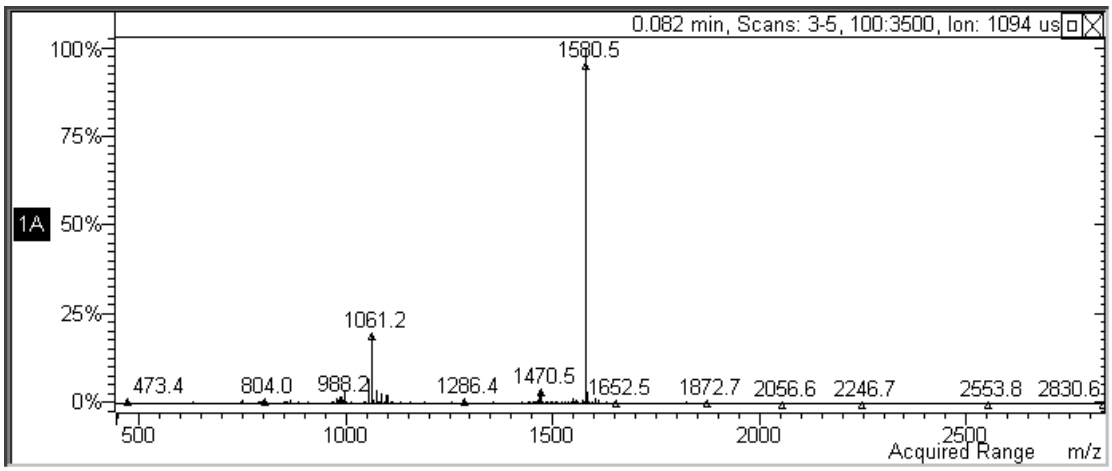

Fig. S11 Electrospray ionization mass spectrum of a mixture of **P5** and **M**. The peak at *m*/*z* 1580.5 is corresponding to $[\mathbf{P5}\supset\mathbf{M} - Br - PF_6]^{2+}$.

4. Critical aggregation concentration (CAC) determination

Some parameters such as the conductivity, osmotic pressure, fluorescence intensity and surface tension of the solution change sharply around the critical aggregation concentration. Here, the dependence of the fluorescence intensity at 471 nm *vs*. solution concentration was used to determine the critical aggregation concentration (CAC). When the concentration of **PTPE** (or **P5-PEG-Biotin⊃PTPE**) is lower than the CAC value, the fluorescence intensity increased slowly. However, fluorescence intensity increased sharply when the concentration was higher than the CAC value due to the AIE effect arising from the self-assembly of **P5-PEG-Biotin⊃PTPE**. Therefore, the junction of the fluorescence intensity at 471 nm-concentration plot represents the CAC value.

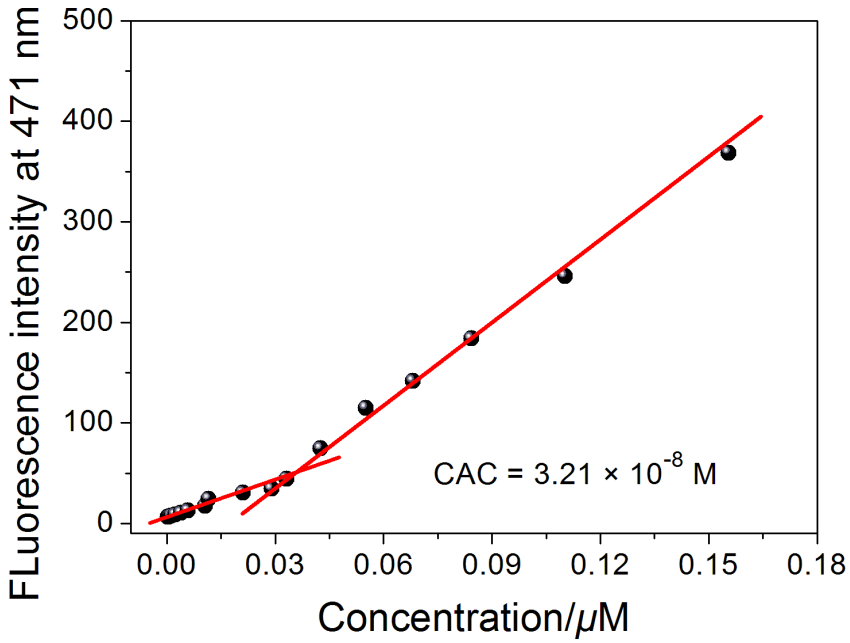

Fig. S12 Plot of the emission intensity at 471 nm *vs*. the concentration of **PTPE**.

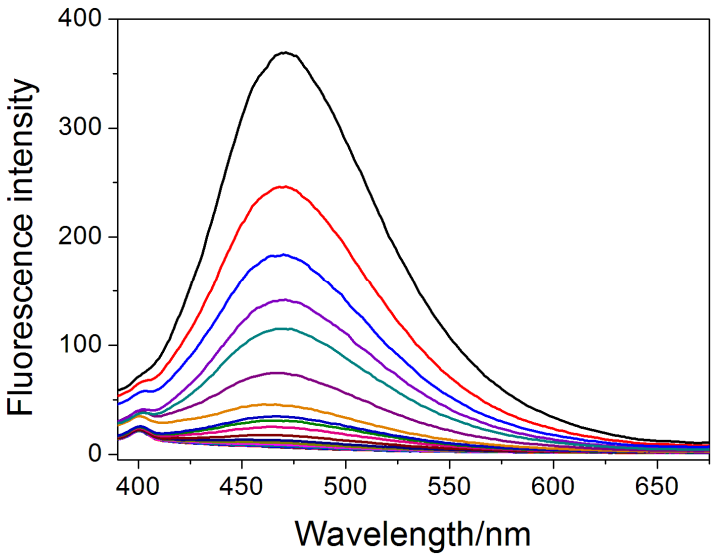

Fig. S13 Fluorescence spectra of **P5-PEG-Biotin⊃PTPE** in water with the TPE unit concentration increasing from 0.116 to 62.2 μM.

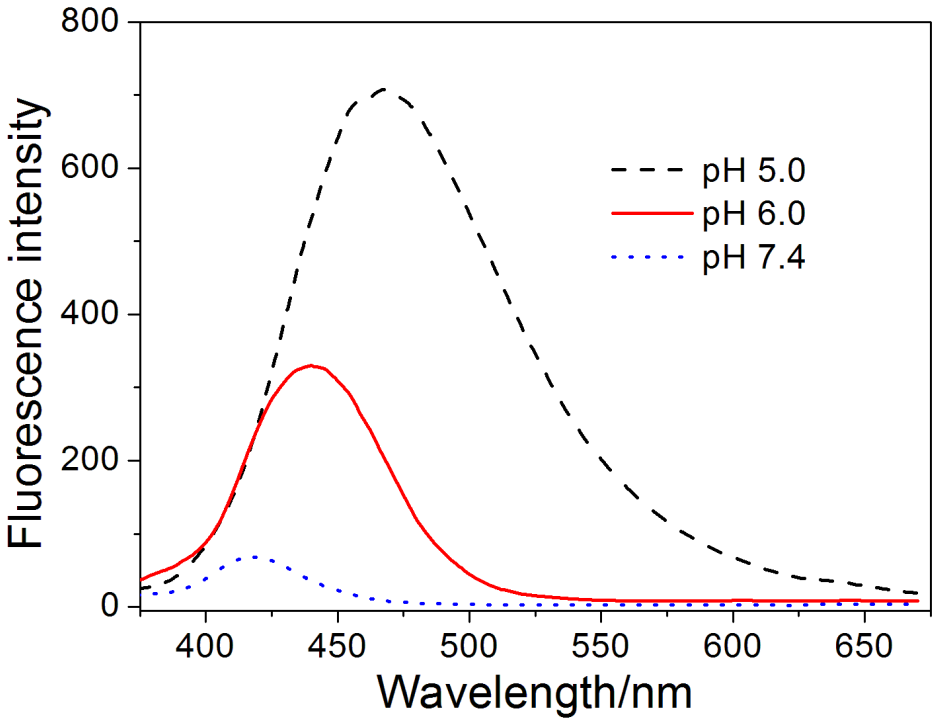

Fig. S14 Recovery of **PTPE** fluorescence by culturing DOX-loaded **SNPs** in PBS at different pH values.

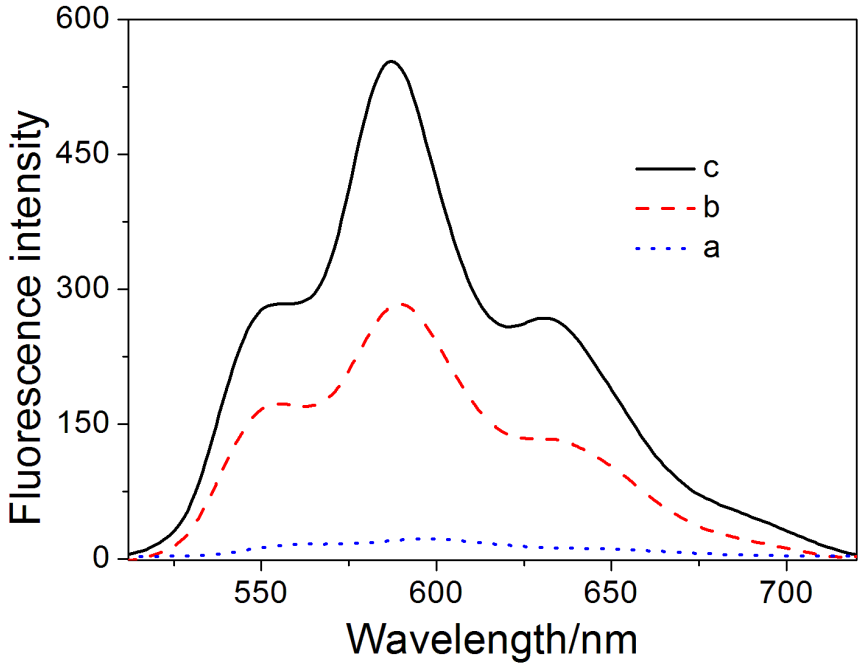

Fig. S15 Fluorescence spectra of (a) DOX-loaded **SNPs**, (b) DOX-loaded **SNPs** at pH 5.0 for 24 h, and (c) free DOX·HCl.

5. In vivo investigations

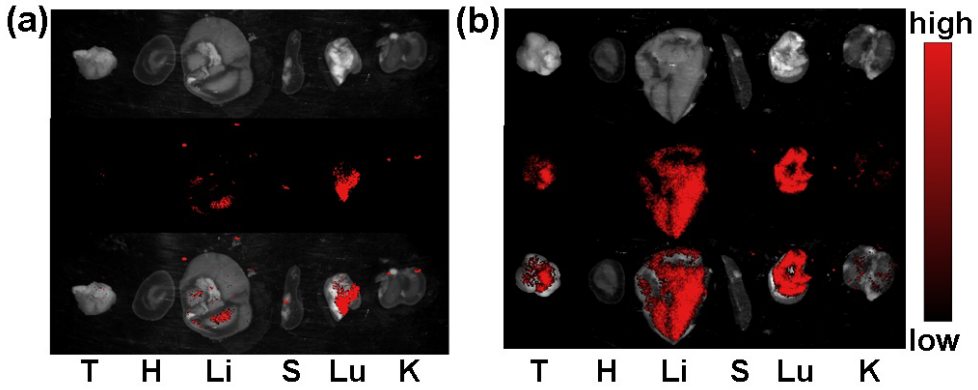

Fig. S16 *Ex vivo* imaging of tumor and major organs for the mice treated with (a) DOX·HCl and (b) DOX-loaded **SNPs** at 24 h post-injection. T: tumor, H: heart, Li: liver, S: spleen, Lu: lung, K: kidney.

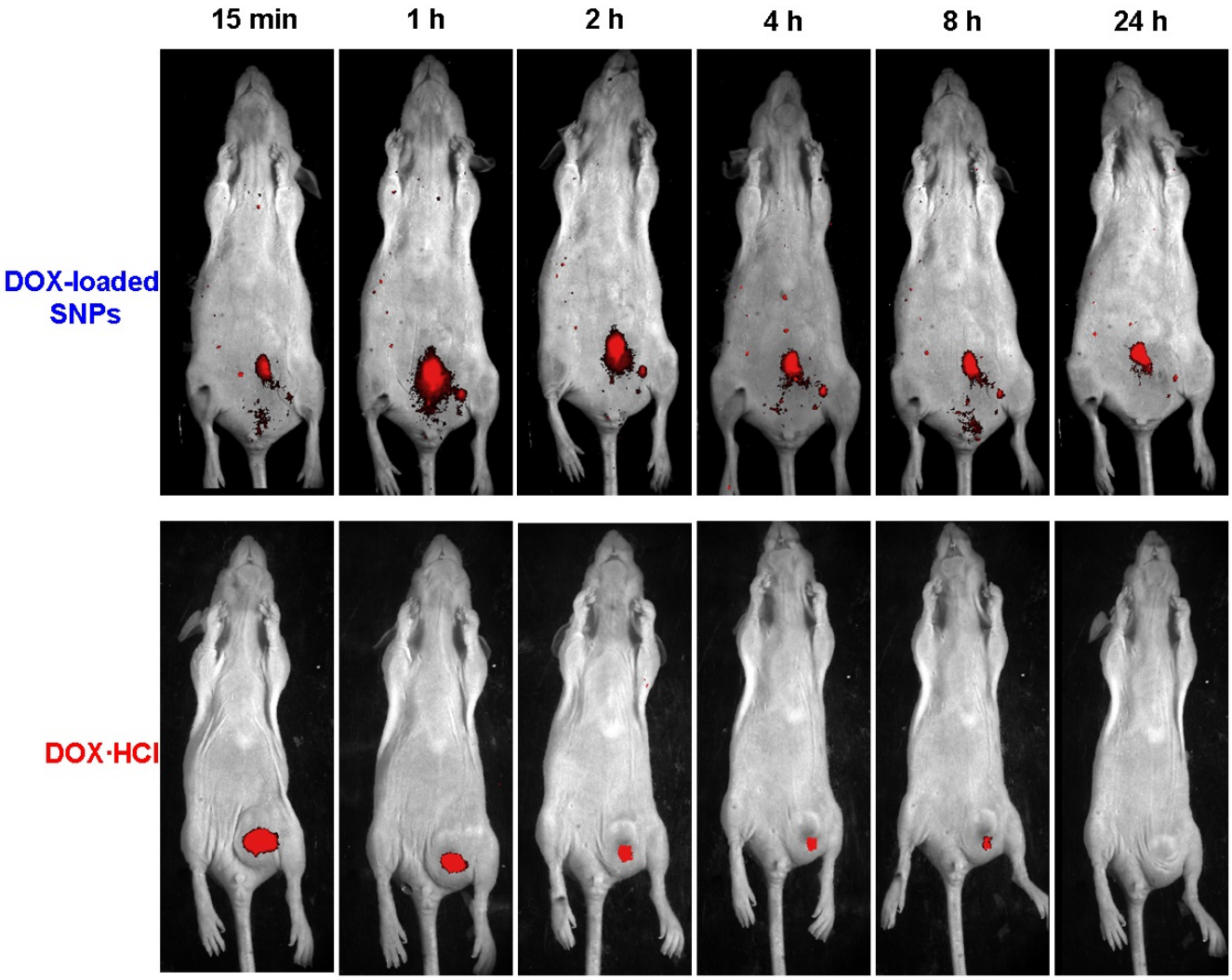

Fig. S17 Time-dependent *in vivo* fluorescence imaging of tumor-bearing mouse treated with free DOX·HCl and DOX-loaded **SNPs**.

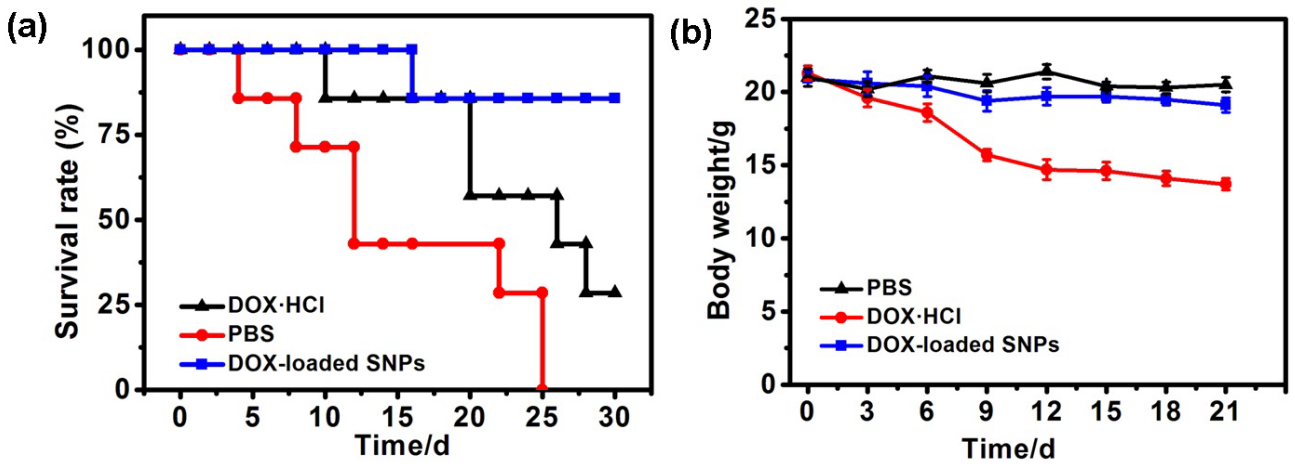

Fig. S18 (a) Survival rate and (b) body weight changes of the mice bearing HeLa tumors after different treatments.

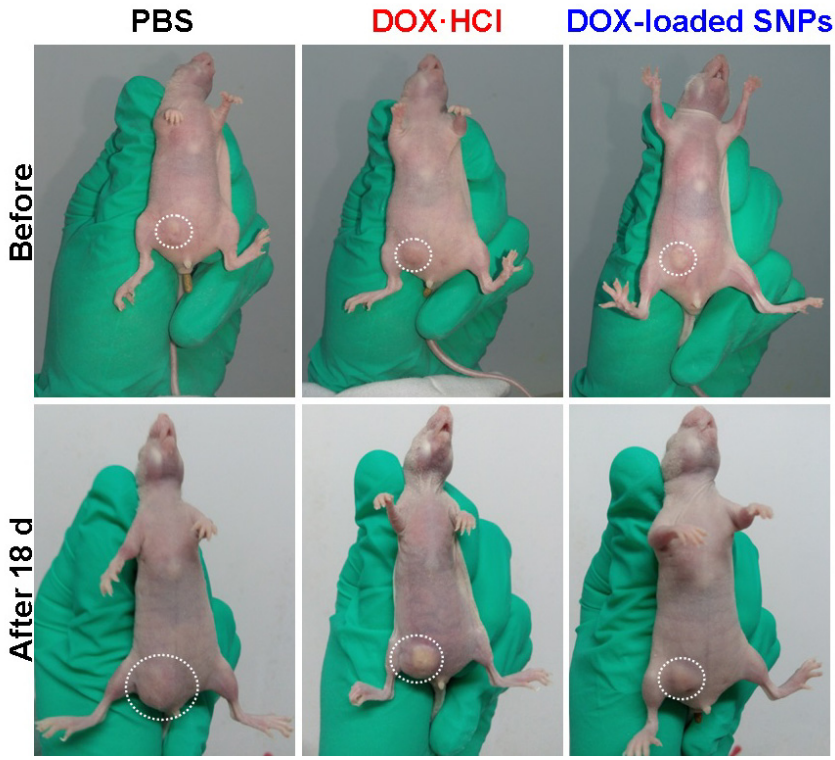

Fig. S19 Photographs of the mice taken before and after 18 days of chemotherapy.

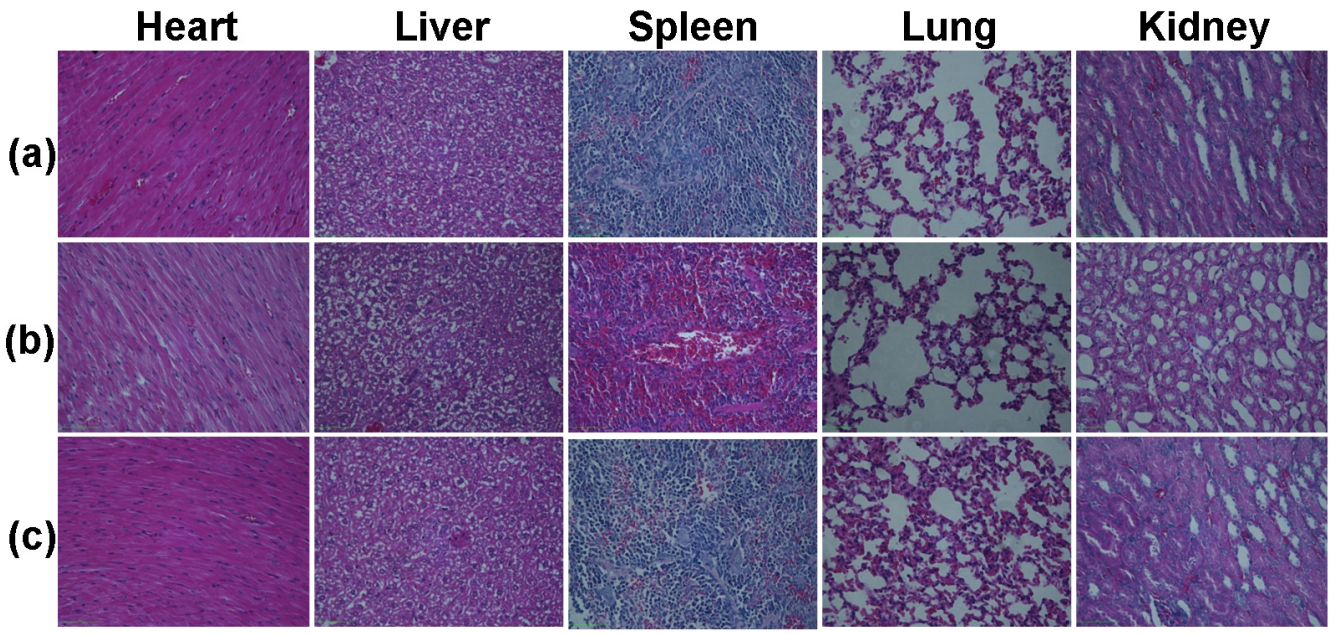

Fig. S20 Histopathologic analysis of major organs after H&E staining, which were harvested from mice treated with (a) PBS, (b) free DOX·HCl, and (c) DOX-loaded **SNPs**.

References:

S1. M. Lamberto, E. E. Rastede, J. Decker and F. M. Raymo, *Tetrahedron Lett*. 2010, **51**, 5618.

S2 X. Ji, Y. Li, H. Wang, R. Zhao, G. Tang and F. Huang, *Polym. Chem*. 2015, **6**, 5021.

S3 G. Yu, W. Yu, L. Shao, Z. Zhang, X. Chi, Z. Mao, C. Gao and F. Huang, *Adv. Funct. Mater*. 2016, DOI: 10.1002/adfm. 201601770.

S4 K. A. Connors, *Binding Constants*, Wiley: New York, 1987. (b) P. S. Corbin, *Ph.D. Dissertation*, University of Illinois at Urbana-Champaign, Urbana, IL, 1999. (c) P. R. Ashton, R. Ballardini, V. Balzani, M. Belohradsky, M. T. Gandolfi, D. Philp, L. Prodi, F. M. Raymo, M. V. Reddington, N. Spencer, J. F. Stoddart, M. Venturi and D. J. Williams, *J. Am. Chem. Soc.*, 1996, **118**, 4931−4951. (d) J. Zhang, F. Huang, N. Li, H. Wang, H. W. Gibson, P. Gantzel and A. L. Rheingold, *J. Org. Chem.*, 2007, **72**, 8935−8938.